Nonlinear Dynamic Processes in an Ensemble of Photosynthetic Reaction Centers. Theory and Experiment

Alexander O. Goushcha,[†] Marina T. Kapoustina,[‡] Valery N. Kharkyanen,[‡] and Alfred R. Holzwarth*,[†]

Max-Planck-Institut für Strahlenchemie, Mülheim a.d. Ruhr, 45470 Germany, and Division of Physics of Biological Systems, Institute for Physics, National Academy of Sciences, Ukraine, Nauki Prospekt 46, Kyiv 252028, Ukraine

Received: March 10, 1997; In Final Form: July 2, 1997[⊗]

The results of a theoretical study of the dynamic self-organization phenomenon in the photosynthetic reaction center (RC) from purple bacteria are presented accounting for the stochastic effects an RC ensembles. The adiabatic approximation is applied to determine the specific role of slow structural (protein/cofactors) modes in the correlated behavior of the electronic and structural variables. It is shown that, at certain values of light intensity, the system undergoes bifurcation. The bistability region for the generalized structural variable occurs where the system has two stable states, one characteristic for the dark-adapted sample (i.e., the sample under very low illumination intensity) and the other for the light-adapted sample. The description is based on the solution of the "forward" Kolmogorov equations using the Markov approach. A distribution function describing the probability of finding the electron localized on a particular cofactor with a certain value of the generalized structural variable is used. Modeling shows a good agreement with the results of experimental investigations of transient optical absorbance changes of the isolated RCs from the purple bacterium *Rhodobacter sphaeroides*. The results indicate that the free energy difference between Q_A^- and Q_B^- changes substantially in different conformational states of the protein/cofactors induced by light over a wide range of the illuminating light intensity.

Introduction

The reaction center (RC) in photosynthetic organisms is a characteristic example of a biological electron transfer system. High-resolution X-ray studies of purple bacterial RCs[1,2] and molecular dynamics simulations of electron transfer (ET) reactions[3,4] have stimulated an increased interest in the physical mechanisms involved in photoinduced ET. The RC is the pigment−protein complex responsible for the primary charge separation in the bacterial photosynthesis. The photoexcitation of a bacteriochlorophyll dimer P (Figure 1) is followed by ultrafast (2−4 ps) charge separation, resulting in formation of the oxidized donor ($P \rightarrow P^+$), with an efficiency close to 100%. During the next stage (∼150−200 ps), the electron transfers to the primary quinone acceptor (Q_A) with essentially the same high efficiency. The subsequent slower stage of ET to the secondary quinone acceptor (Q_B), and its possible further recombination with the hole on the pigment pair P or return to the acceptor Q_A, are of particular interest because the rates and efficiencies of these processes depend strongly on the specific configuration of some flexible structural elements of the protein matrix and cofactors. It has been shown that electron localization on each of the quinone acceptors causes structural changes in the RC[5−7] which strongly influence the efficiency and rates of ET. This feedback action of the rearranged structure on the efficiency of charge transfer may be considered as a correlated dynamics of electronic and structural variables of the system. In this case, the system, from a theoretical point of view, has to be described in terms of stochastic nonlinear dynamic theories.[8] In analogy with other chemical, physical, and biological systems, the appearance and disappearance of new self-organized states or oscillating regimes are possible.[9−11] It was shown in recent publications[12−15] that such a correlated behavior of electronic and structural variables leads to the effect of dynamic self-organization (or, better, self-regulation) in macromolecular charge transfer systems. A theoretical description has been developed which described the situation for a single RC.[12,13] However, this does not account for the stochastic effects in an ensemble of functioning RCs, which is the situation at hand in a real experiment. Such effects, in part, have been taken into account in ref 14, where an exact stochastic description within an approximation of the RC as a two-level system was presented. The authors described there the processes of RC turnover as a dichotomous noise process. Nevertheless, a more detailed approach to describe the real functioning system is necessary for understanding the dynamics of an ensemble of

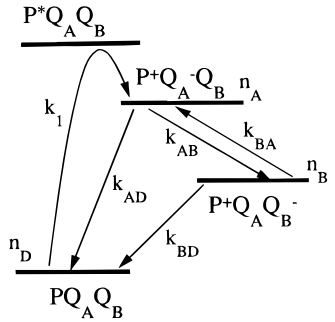

Figure 1. Electron transfer (ET) scheme for the RC from purple bacteria *R. sphaeroides*. PQ_AQ_B is the state with an unexcited bacteriochlorophyll dimer P, whereas $P^+Q_A^-Q_B$ and $P^+Q_AQ_B^-$ are the states with an electron localized on the primary and secondary quinone acceptors, respectively. The short-lived states with electron localization on bacteriopheophytin and bacteriochlorophyll monomer are not shown. n_P, n_A, and n_B are the populations of the corresponding levels, respectively.

* To whom all correspondence should be addressed. Fax: (+49)208 306 3951. E-mail: Holzwarth@mpi-muelheim.mpg.de.
† Max-Planck-Institut für Strahlenchemie.
‡ National Academy of Sciences, Ukraine.
⊗ Abstract published in *Advance ACS Abstracts,* August 15, 1997.

S1089-5647(97)00868-7 CCC: $14.00

RCs. The complex nonlinear dependencies and hysteresis effects observed for the RC absorbance changes[12,16,17] and the dependence of the primary donor re-reduction kinetics[18−20] on various conditions of optical excitation were taken as evidence for dynamic self-regulation. In this work, we present a self-consistent stochastic description of the ensemble of macromolecules undergoing ET, and we demonstrate the importance of nonlinear dynamic effects in the experimentally observed dependencies.[17] We shall start by developing a theory for the correlated movement of the photoelectron and the RC protein/cofactor conformation in a three-level model and then apply the model to experimental data obtained on RCs from the purple bacterium *Rhodobacter sphaeroides* (*R. sphaeroides*).

Theory

Let us consider an ensemble of isolated RCs carrying both primary and secondary quinone acceptors (Q_A and Q_B). The later steps of electron tunneling as well as recombination from both acceptors are of dominant interest for us. In this case, we can neglect the populations of primary charge-separated states, i.e., states with an electron localized either on the bacteriochlorophyll monomer or on the bacteriopheophytin molecule, and consider a simpler three-level model for the RCs (Figure 1).

A set of functions $P_i(t,x)$ defining the coupled (in terms of electron i and structural x coordinates) probability of electron localization on the i binding site (i = D, A, B; here, A and B denote the primary or the secondary acceptors, and D denotes the primary electron donor) of the RC with a generalized structural variable x, at time t, will be used for the statistical description of the entire RC ensemble. We use the "forward" Kolmogorov equations[21,22] for determining $P_i(t,x)$ using the Markov approach:[23]

$$\frac{\partial P_D(t,x)}{\partial t} = \hat{L}_D P_D(t,x) - k_1 P_D(t,x) + k_{AD} P_A(t,x) + k_{BD} P_B(t,x)$$

$$\frac{\partial P_A(t,x)}{\partial t} = \hat{L}_A P_A(t,x) + k_1 P_D(t,x) - (k_{AD} + k_{AB}(x)) P_A(t,x) + k_{BA}(x) P_B(t,x) \quad (1)$$

$$\frac{\partial P_B(t,x)}{\partial t} = \hat{L}_B P_B(t,x) - k_{BA} P_B(t,x) + k_{AB}(x) P_A(t,x) - k_{BD} P_B(t,x)$$

where

$$\hat{L}_i = C_d \frac{\partial}{\partial x}\left[\frac{1}{K_b T}\frac{\partial V_i(x)}{\partial x} + \frac{\partial}{\partial x}\right] \quad (2)$$

$V_i(x)$ is the potential of the structural variable x in the case of electron localization on the i binding site, and C_d is a diffusion constant corresponding to the movement of the generalized structural variable x on the potential surface. Several experiments (see, e.g., refs 12, 17, 20, and 24) show that photoactivation of RCs leads to reversible structural changes, which relax more slowly than the recombination time of the distribution of the charge-separated states. In this case, the ET between cofactors will be of adiabatic character, and the kinetic constants k_i (Figure 1) will depend parametrically upon such slow structural changes. In our treatment, we will take into account (see below) the dependence of only two rate constants, k_{AB} and k_{BA}, on the single "slowly varying" structural variable x. Such an approximation should be reasonable for the photosynthetic RC because these rate constants change drastically (as was shown experimentally for the *R. sphaeroides* RC[25]) under the variation of the experimental conditions (temperature, actinic light intensity, etc.).

A number of studies[3,26,27] have shown the significance of fast structural dynamics in the description of a functioning RC. With respect to such fast structural changes, the electron transfer can be treated as nonadiabatic. The influence of these fast structural variables is typically included in the expressions for the ET rates in accordance with the well-known Marcus expression for the (nonadiabatic) ET rates.[28,29]

Our model (eqs 1 and 2) may be considered as the generalization of the Agmon−Hopfield model[30] for the case of three states of the main system coordinate (population probabilities P_D, P_A, and P_B of the states PQ_AQ_B, $P^+Q_A^-Q_B$, and $P^+Q_AQ_B^-$, respectively) accounting for all possible transitions between them.

A general solution of the system eqs 1 and 2 cannot be derived without an additional simplification. If we take into account that the relaxation of the RC electronic coordinate occurs much faster than the structural one, the solutions to eqs 1 and 2 can be given in the adiabatic approximation:

$$P_i(t,x) = n_i(t|x) P(t,x) \quad (3)$$

$$\frac{\partial P(t,x)}{\partial t} = C_d \frac{\partial}{\partial x}\left[\frac{P(t,x)}{K_b T}\frac{\partial V_{eff}(x)}{\partial x} + \frac{\partial P(t,x)}{\partial x}\right] \quad (4)$$

where $n_i(t|x)$ is the population at the binding site i with a fixed generalized structural variable x, which is averaged over the fluctuation caused by an electronic transition. This structural variable x can be considered as a control mode;[31] $P(t,x)$ is the probability density to find the RC with the generalized structural variable x at a particular electron localization site i; $V_{eff}(x)$ is an effective adiabatic nonequilibrium potential for the control mode x, determined from

$$\frac{\partial V_{eff}(x)}{\partial x} = \sum_i \frac{\partial V_i(x)}{\partial x} n_i(x); \quad n_i(x) = \lim_{t\to\infty} n_i(t|x) \quad (5)$$

The effective potential is of statistical origin (i.e., it depends on the populations n_i) and depends upon the intensity I of the actinic light due to the dependence of $n_i(t|x)$ on I. The light intensity I (actually, the light-induced turnover rate) in this case stands for the control parameter of the nonequilibrium potential and, therefore, determines the nonlinear dynamic behavior of the system.[31] We will now show that bifurcation can arise for the system under consideration.

The eqs 3 and 4, together with eq 5 and the balance equations for the population probabilities $n_i(t|x)$ (see below, eq 7, for the time-dependent populations of binding sites i; we omitted in these equations the brackets $(t|x)$ near each of the symbols n_i for simplicity), give the correct general description for an ensemble of RCs. This accounts for the effects of the interaction of the photoactivated electron with the adiabatic structural variable x. One should note that eq 4 for the RC ensemble corresponds to the stochastic equation for the structural variable x of a single RC, which can be given by[8]

$$\tau_x \frac{dx}{dt} = -\frac{\partial V_{eff}(x)}{\partial x} + \sqrt{2C_d}\zeta(t) \quad (6)$$

where x is averaged over the fluctuations caused by an electronic transition, as indicated above (that is, x in both eqs 4 and 6 should be considered as averaged over a time interval longer than the time of charge recombination but shorter than the

relaxation time of the adiabatic structural variable x); $\zeta(t)$ describes a δ-correlated random process which models the initial thermal fluctuations of the structural variable of a single RC and $\tau_x = k_b T/C_d$. The theory for a single RC was developed earlier in refs 12 and 13, where the stochastic term $(2C_d)^{1/2}\zeta(t)$ has been neglected. The approach used in previous work corresponds to the particular case, described also in the present paper, when the RCs distribution function over the structural variable is very narrow. Then, as will be shown below, we can introduce the simplified *conformational approach* (see, e.g., ref 32), assuming that, in a particular *conformational state* (which corresponds to a maximum of the distribution function $P(t,x)$), the RCs have almost equal values of the structural variable.

Next, we consider the time evolution of the populations of the different RC levels. This can be described by the following system of balance equations relating to the scheme in Figure 1:

$$\frac{dn_D}{dt} = -k_1 n_D + k_{AD} n_A + k_{BD} n_B$$

$$\frac{dn_A}{dt} = -k_{AD} n_A - k_{AB} n_A + k_1 n_D + k_{BA} n_B \qquad (7)$$

$$\frac{dn_B}{dt} = +k_{AB} n_A - k_{BA} n_B - k_{BD} n_B$$

with normalization conditions

$$n_D + n_A + n_B = 1 \qquad (8)$$

In eq 7, k_1 is proportional to the intensity of the actinic light, I; k_{AD} can be taken as a constant for the sake of simplicity. A dependence of the rate constant k_{AD} on the light intensity for the samples containing only the primary (Q_A) acceptors has been found recently,[20,33] and it was shown in ref 12 that this can be due to a small light-induced structural change that has no pronounced influence on other macroscopic parameters of the RC. The k_{AD} value can be determined from experiments;[5,25] likewise, $k_{AB}/k_{BA} = \exp(\Delta G_{AB}/k_b T)$ can be determined from experiment,[34−36] where ΔG_{AB} is the energy difference between the $P^+Q_A^-Q_B$ and $P^+Q_AQ_B^-$ states, k_b is the Boltzmann constant, and T is the temperature. According to ref 35, we can also set $k_{BD} = 0$, reflecting a negligible probability of a direct pathway for recombination, as compared to the recombination $P^+Q_AQ_B^- \rightarrow PQ_AQ_B$ via the primary acceptor Q_A.

Next, we need to find a suitable macroscopic parameter of the RC to describe the correlation between the ET rate constants and the light-induced structural changes. Taking into account the dependence of ΔG_{AB} on the RC structure (see, for example, refs 34−39, where k_{AB}, k_{BA}, and ΔG_{AB} were determined under different experimental conditions which influence the protein/cofactor structure), we will describe, for the sake of simplicity, the RC structural changes in terms of their influence on the free energy difference ΔG_{AB} between the states $P^+Q_A^-Q_B$ and $P^+Q_AQ_B^-$ only. In such a description, we assume that $\Delta G_{AB} = \varphi(x)$, where φ is some function of the structural variable x. The structural changes following electron localization on the quinone acceptors Q_A and Q_B are likely to be very complex. As an example, we can mention the fast protonation of protein groups which are close to the quinone acceptors, the stronger binding of the singly reduced quinone to the protein pocket as compared to the oxidized one, and the slow conformational rearrangements of the binding pocket itself, which relax on a time scale of minutes.[20,24] We consider in our theoretical model that the slow conformational rearrangements which influence the value of ΔG_{AB} can be described in terms of a single generalized structural variable x. Such a variable may describe the complex reorganization of the system and can be introduced in a similar way as the generalized "reaction coordinate" (or "perpendicular coordinate" [30]) in chemical kinetics. We assume also that ΔG_{AB} is a single-valued function of the structural variable. Hence, for the present consideration, we choose the simplest, i.e., linear relation between ΔG_{AB} and x without any restriction of generality. We thus take $x = \Delta G_{AB}/k_b T$ as a dimensionless coordinate. Equations 1−6 then describe the dynamics for this structural variable. The stationary populations $n_A(x)$ and $n_B(x)$ (for their definitions see eq 5) can be defined as functions of both actinic light intensity I and structural variable x. Following these lines, the expressions for populations $n_A(I,x)$ and $n_B(I,x)$ can be easily derived from the balance equations taking into account eq 8:

$$n_A(I,x) = \frac{I}{I(1 + \exp(x)) + k_{AD}}; \qquad n_B(I,x) = \frac{I \exp(x)}{I(1 + \exp(x)) + k_{AD}} \qquad (9)$$

where we assumed that $k_1 \equiv I$ (both these quantities as well as other rate constants are given in s^{-1}).

Let us consider the changes of the effective potential $V_{eff}(x)$ for the three-level system indicated in Figure 1 under the variable actinic light intensity I. In this case, we can write $V_{eff}(x) \equiv V_{eff}(x,I)$ (note that the function $V_{eff}(x,I)$ is the same function as $V_{eff}(x)$, with the only difference that the first is written using the direct representation of the dependence on I, whereas the second one has this dependence hidden in x). The potential $V_{eff}(x,I)$ is determined from eq 5 by accounting for the condition

$$n_A(I,x) \ll n_B(I,x),\ n_P(I,x) \qquad (10)$$

which follows directly from both the relationship (9) and the inequality $k_{AB}/k_{BA} = \exp(x) \gg 1$. (The inequality (10) is always valid except for the case of the saturating intensities of pulsed RCs photoactivation when $n_A(I,x) \approx 1$ just after the initial steps of the charge separation. Such a situation does not apply to our situation; thus, the correlation (10) is valid for all values of I and x that are of interest.) The low value of the population $n_A(I,x)$ under the conditions assumed here means that the light-induced structural changes in the Q_A binding pocket are much less probable than those in the Q_B binding pocket.[45] We thus restrict the consideration to the structural changes of only the Q_B pocket in view of presently available experimental data (see also the discussion below). This means that the structural variable $x = \Delta G_{AB}/k_b T$ is determined mainly by the local structure around the Q_B site. This may be justified by several arguments. First, the polarity of the Q_B pocket is much larger than that of the Q_A pocket.[40] This favors the conditions where the photoinduced charge separation influences the local structure in the Q_B site by electrostatic interactions more than in the Q_A site. Second, the binding strength of ubiquinone in the Q_B site depends strongly on the Q_B redox state.[41,42] Third, the lifetime of the $P^+Q_AQ_B^-$ state is considerably longer than the lifetime of all other charge-separated states in the RC, which allows for a higher effective influence of the electron charge on the surrounding structure. Thus, we can omit for simplicity in eq 5 the term $\partial V_A(x)/\partial x\ n_A(I,x)$ and, using eqs 5, 8, and 10, obtain an expression for the effective potential $V_{eff}(x,I)$:

$$\frac{\partial V_{eff}(x,I)}{\partial x} = \frac{\partial V(x)}{\partial x} - f_B n_B(I,x) \qquad (11)$$

where $V(x) \equiv V_D(x)$ is the initial potential when the electron is localized on the donor and

$$f_B = \left(-\frac{\partial V_B(x)}{\partial x}\right) - \left(-\frac{\partial V_D(x)}{\partial x}\right) \quad (12)$$

where f_B is an additional force acting on the structural variable only in the case of an electron being localized on Q_B. We will use in the further calculations the f_B value in units of k_bT. This force f_B is of stochastic nature, and it describes the perturbation of the local RC structure in the $P^+Q_AQ_B^-$ state.

For the sake of simplicity but without losing generality, we will use the constant force approximation so that f_B does not depend on x. An initial effective potential $V(x)$ should be chosen for the determination of the dependence of the structural variable x on the intensity of the actinic light. We will take the harmonic potential $V(x) = k(x - x_0)^2/2$, where k is given in energy units and depends on the medium elasticity (k is defined usually as the quantity which essentially depends on the solvent reorganization energy; see, e.g., ref 43), and x_0 (a dimensionless value) is the equilibrium value of the structural variable in the absence of actinic light (when electron is on P). Then we obtain from eqs 11 and 12

$$\frac{\partial V_{eff}(x,I)}{\partial x} = k(x - x_0) - f_B n_B(I,x) \quad (13)$$

After integrating eq 13 and taking into account eq 9, we get

$$V_{eff}(x,I) = \frac{k(x - x_0)^2}{2} - k(x_B - x_0)\ln\frac{(1 + \exp(x))I + k_{AD}}{(1 + \exp(x_0))I + k_{AD}} + C(I) \quad (14)$$

where $(x_B - x_0) = f_B/k$ denotes the maximum shift of the structural variable that could occur under the limiting condition of permanent localization of an electron on Q_B; $C(I)$ is an integration constant which depends primarily on the intensity of actinic light. It is easy to show (taking into account initial conditions) that

$$C(I) = \frac{f_B^2}{2k}\left[\frac{I\exp(x_0)}{I(1 + \exp(x_0)) + k_{AD}}\right]^2 \quad (15)$$

From the analysis of eq 14, we obtain, for the case that the condition

$$x_B - x_0 \geq 4 \quad (16)$$

is fulfilled, two minima in the effective potential $V_{eff}(x,I)$ (see below).

Figure 2 shows the calculated dependencies of $V_{eff}(x,I)$ in the model described above for RCs from *R. sphaeroides* at different values of the actinic light intensity I. The minima of the effective potential correspond to the stable states of the system. We will denote these states as *conformational states*, where the corresponding values of the structural variable x will be termed as *conformational coordinate* value, χ. We should note here that the initially introduced quantity x in the Fokker–Planck equation (eq 1) has the meaning of a generalized structural variable for which we have developed the above formalism. The manifold of the states of the electronic–conformational system of the RC can be characterized in general by the manifold of values x. The conformational coordinate χ, in contrast, describes only the equilibrium configurations of the

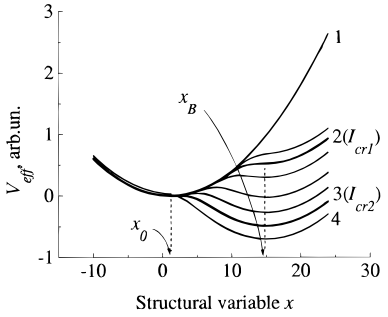

Figure 2. System conformational potential obtained for $(x_B - x_0) = 13$ under different levels I of stationary actinic light: 1, 0; 2, 10^{-4} (Icr_1); 3, 1.5×10^{-1} (Icr_2); 4, 1. The curve between 1 and 2 and all the curves between 2 and 3 correspond to intermediate I levels. The second potential minimum appears at $Icr_1 = 10^{-4}$ (the bifurcation point). The value $I = 1$ corresponds to the half-saturating light intensity, ca. 2×10^{15} quanta/(cm^2 s). $x_B = f_B/k + x_0$ is the conformational coordinate value after passing the second bifurcation point (at high actinic light intensity). x_0 is the conformational coordinate value in the absence of light (see text). The curves were obtained for the following values of the RC parameters: $k_{AD} = 13$; $f_B = 7$; $k = 0.5$; $x_0 = 1$ (k_{AD} is in the same units as I, s^{-1}; f_B and k are in the units of k_bT; x_0 is dimensionless).

conformational system. This means that the values x and χ are identical only for the manifold of equilibrium states when the first derivative of the effective adiabatic potential equals zero (see below). Note that, in this definition, the above-introduced quantities x_0 and x_B belong to the manifold of the conformational coordinate χ values (we will nevertheless use for these two particular characteristic parameters the structural variable value of the dark-adapted RCs and the maximal shifted structural variable value, the previously introduced symbols x_0 and x_B, respectively). We now proceed with the development of the theory using the *conformational* approach.[32] According to the description given above, the equation for determination of the conformational coordinate values χ may be obtained from $\partial V_{eff}(x,I)/\partial x|x{=}\chi = 0$:

$$\chi = x_0 + \frac{f_B}{k}\frac{I\exp(\chi)}{I(1 + \exp(\chi)) + k_{AD}} \quad (17)$$

From the analysis of the dependence $\chi(I)$, two cases should be distinguished. The first corresponds to the case of weak interaction between the electron localized on Q_B and the local structure in the Q_B site. In this case, the structural changes are not large enough (i.e., the difference $(x_B - x_0)$ would be less than the critical value) to ensure efficient feedback in the electronic–conformational system of the RC. The function $\chi(I)$ in this case grows monotonical and simultaneously with increasing I and approaches asymptotically a constant value at $I \rightarrow \infty$ (this rather trivial case is not shown in Figure 3). In the second case (i.e., the strong interaction case when the maximal possible structural change described by the difference $(x_B - x_0)$ exceeds the critical value), which is of primary interest for us, the dependence is of *S-type* in shape (see Figure 3). As indicated earlier, such a dependence is typical for the behavior of the reaction coordinate of systems under conditions far from thermodynamic equilibrium.[9−11,31] This means that one should expect, in such a situation, the characteristic nonlinear dynamic effects (synergetic effects[9−11,31]) in the behavior of certain RCs parameters under particular conditions of actinic illumination. In particular, bifurcations should be observable in this case, and they should appear for RCs if $(x_B - x_0) \geq 4$ (see Figure 3). The values of the *conformational coordinate* which correspond to the two bifurcation points (where the derivative $\partial I/\partial\chi = 0$) are determined from eq 17 as

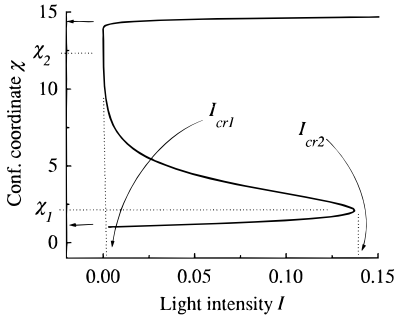

Figure 3. Dependence of the conformational coordinate values χ on the actinic light intensity for the case $(x_B - x_0) = 13$. Icr_1 and Icr_2 are the intensities of the light corresponding to the bifurcation points χ_1 and χ_2 of the system (see text). Two horizontal arrows indicate the value of conformational coordinate in the dark (x_0, lower value) and under saturation light intensity (x_B, upper value). The curve was obtained for the following values of RC parameters: $k_{AD} = 13$; $f_B = 7$; $k = 0.5$; $x_0 = 1$ (k_{AD} is in the same units as I, s^{-1}; f_B and k are in the units of k_bT; x_0 is dimensionless).

$$\chi_{1,2} = \frac{x_B + x_0}{2} \pm \sqrt{\left(\frac{x_B - x_0}{2}\right)^2 - (x_B - x_0)} \qquad (18)$$

Hence, it follows that, at $(x_B - x_0) < 4$, the bistability region is absent, and the weak interaction case described above is realized. Note the close proximity of the values χ_1 and χ_2, which denote the bifurcation points, to the values x_0 and x_B, which denote the *conformational coordinate* values in the dark and at saturating actinic light, respectively, for the case $(x_B - x_0) \geq 4$ (see Figures 2 and 3). This proximity is due to the particular type of adiabatic potential that has been chosen in the present consideration. This means also that an increase of the light intensity above Icr_2 (see Figure 2) causes only minor further changes of the conformational coordinate value as compared to its value χ_2 in the upper bifurcation point (see below). Analogously, the decrease of the light intensity below Icr_1 causes also only slight changes of the conformational coordinate value as compared to its value χ_1 in the low-intensity bifurcation point.

In the case of strong electronic−conformational interaction and feedback in the system, i.e., when $(x_B - x_0) \geq 4$, the RCs are described by an adiabatic potential with only one minimum at $I < 10^{-4}$ (see curve 1 and the curve between 1 and 2 in Figure 2). The second potential minimum (curve 2 in Figure 2) characterizes the new *conformational state* of the system appearing at the bifurcation point ($Icr_1 \approx 10^{-4}$). The latter can be seen in the χ dependence on actinic light intensity (Figure 3). After passing a critical value, Icr_1 (the bifurcation point), the system is characterized by three possible stationary states. Two of them (upper and lower branches in Figure 3) are stable and correspond to the potential minima. The third state is unstable and corresponds to the maximum of the potential. After passing the second bifurcation point, $Icr_2 \approx 1.5 \times 10^{-1}$, the system remains in the single allowed (light-adapted) state with a considerably displaced *conformational coordinate* χ as compared to that in the dark state.

From the above discussion, it follows that the RC *conformational coordinate*, which represents the control mode for fast electronic transitions, should reveal a nontrivial dependence on actinic light intensity (if $(x_B - x_0) \geq 4$, the validity of such a correlation for purple bacteria RCs will be discussed below). The χ coordinate value increases slowly with an increase of the actinic light intensity from 0 to Icr_1. In the region $Icr_1 < I < Icr_2$, two different *conformational states* coexist with essentially different values of the *conformational coordinate* χ. Using detailed balance of the states connected by the rate constants k_{AB} and k_{BA} (dependent on the variable x), the different values of these rate constants will correspond to different RC conformational states in the bistability region. For the case $I > Icr_2$, the *conformational coordinate* has a single value and is almost independent of I. Note that, under the conditions of decreasing actinic light intensity back into the bistable region down to the Icr_1, the *conformational coordinate* remains unchanged if the thermally activated transitions between the minima of the adiabatic potential do not succeed in equilibrating thermodynamically the RC conformational states during the variation of I.

From the considerations made above, it can be concluded that the behavior of the electronic−conformational system of the RCs may depend strongly on the prehistory of photoactivation, i.e., the turnover rate. Nonlinear dynamic effects should become significant and can be observed experimentally when the relationship (16) is fulfilled, i.e., when $\Delta G_{AB}(I = \infty) - \Delta G_{AB}(I = 0) > 4k_BT$. As was shown in recent publications,[12,16,17] this correlation should, indeed, be fulfilled for the purple bacterial RC. One should note, however, that, in accordance with the results of the theory presented here, the measurement of the value $\Delta G_{AB}(I = \infty)$ should be carried out after prolonged illumination of the RCs with light of saturating intensity, such that the relaxation of the conformational coordinate is complete.

Modeling and Experimental Results

To allow comparison with experiment, we develop the theory further to describe the behavior of a macroscopically accessible parameter of the RCs ensemble, i.e., the optical absorbance change of P.

Let us consider the change of the RC ensemble distribution over the structural variable in two limiting cases of variation of the actinic light: (a) a slow adiabatic variation of I, which permits thermodynamic equilibrium to be reached between the conformational states of the system, and (b) a nonadiabatic variation of I, in which the thermodynamic equilibrium is reached near each of two minima of the effective potential $V_{eff}(x,I)$ independently. In the latter case, we assume that the height of the barrier between the two potential minima is large enough that we may neglect the thermally activated system transitions between *conformational states* during the period of variation of the actinic light intensity I.

Let N be the total number of RCs. The Boltzmann distribution can be written for the density of states of the structural variable under stationary conditions for the fully thermodynamically equilibrated system:

$$P(x) = Z^{-1} \exp(-V_{eff}(x,I)/k_bT);$$
$$Z = \int_{-\infty}^{\infty} \exp(-V_{eff}(x,I)/k_bT)\, dx \qquad (19)$$

This case is realized when the rate of light intensity variation is very slow in comparison with the rate of the thermal transitions over the potential maximum. Then the thermally equilibrated system distribution has time to establish itself at each new value of actinic light intensity. The prehistory of the intensity variation does not influence the distribution in that case.

Another extreme case is realized when the thermal transitions over the potential barrier can be neglected (fully nonequilibrium case). This means that the proper quasi-stationary distribution is reached for each of the two potential minima independently. The potential maximum at $x = x_{max}$ divides the total RC number N into two parts, $\nu 1N$ and $\nu 2N$, where $\nu 1$ and $\nu 2$ are the populations of the RC conformational states. The number of RCs with $x < x_{max}$ is $\nu 1N$, whereas the corresponding number

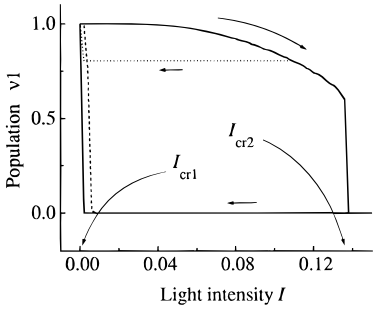

Figure 4. Plot of the RC population $\nu 1$ in the first potential minimum as a function of actinic light intensity for the case far from thermodynamical equilibrium (solid and dotted lines) and the thermodynamical equilibrium case (dashed line). The dotted line is plotted for the case $I_{max} < Icr_2$, whereas the solid and dashed curves are obtained for $I_{max} > Icr_2$ (see text). The arrows show the direction of light intensity alteration. The values of parameters used for the calculations are the same as in Figures 2 and 3.

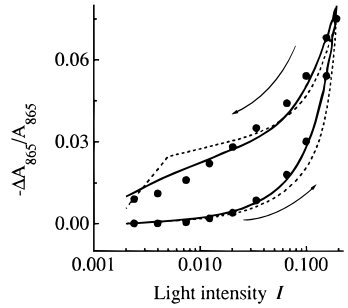

Figure 5. Experimental (dots) and theoretical (solid and dashed curves) dependencies of optical absorbance changes for the RCs from *R. sphaeroides* on variation of the intensity of actinic light. The theoretical curves were obtained for the following parameters values: (1) $k_{AD} = 13$, $x_0 = 1$, $k = 0.5$, and $f_B = 7$ (the solid line) and (2) $k_{AD} = 6$, $x_0 = 1$, $k = 1.8$, and $f_B = 10$ (the dashed line) (k_{AD} is in the same units as I, s^{-1}; f_B and k are in the units of k_bT; x_0 is in dimensionless). $\Delta A_{865}/A_{865} = 0$ corresponds to the system in the dark. The horizontal intensity scale I is given as the fraction of the half-saturating light intensity level $I = 1$ (corresponding to the photon flux, 2×10^{15} quanta/(cm^2 s). The arrows on the plots show the direction of actinic light intensity variation.

with $x > x_{max}$ is $\nu 2N$. The boundary conditions for these cases are as follows: at $I = 0$, $\nu 1 = 1$ and $\nu 2 = 0$; at $I > Icr_2$, $\nu 2 = 1$ and $\nu 1 = 0$. The resulting distribution function for the non*equilibrium case* can be simplified, and we obtain

$$P(x) = \begin{cases} \nu 1 Z_1^{-1} \exp\left(\dfrac{-V_{eff}(x,I)}{k_bT}\right), \\ \qquad Z_1 = \displaystyle\int_{-\infty}^{x_{max}} \exp\left(\frac{-V_{eff}(x,I)}{k_bT}\right) dx, \quad x < x_{max} \\ (1-\nu 1) Z_2^{-1} \exp\left(\dfrac{-V_{eff}(x,I)}{k_bT}\right), \\ \qquad Z_2 = \displaystyle\int_{x_{max}}^{\infty} \exp\left(\frac{-V_{eff}(x,I)}{k_bT}\right) dx, \quad x > x_{max} \end{cases} \tag{20}$$

If I rises from Icr_1 to Icr_2 (cf. Figure 3), then $\nu 1$ decreases in accordance with

$$d\nu 1(I) = Z_1^{-1} \exp\left(\frac{-V_{eff}(x_{max},I)}{k_bT}\right) \nu 1 \, dx_{max} \tag{21}$$

whereas $\nu 2$ increases by the same amount.

If I decreases from Icr_2 to Icr_1, then $\nu 1$ increases,

$$d\nu 1(I) = Z_2^{-1} \exp\left(\frac{-V_{eff}(x_{max},I)}{k_bT}\right) (1-\nu 1) \, dx_{max} \tag{22}$$

and $\nu 2$ decreases by the same amount.

The dependence of the population $\nu 1$ of the first *conformational state* upon the actinic light intensity for the system without thermal transitions is shown in Figure 4 (solid line). The dependence is of a characteristic hysteresis type with large width if the activating light intensity in its maximum (I_{max}) is close to or exceeds the value Icr_2 (Figure 4, solid line). The width of the hysteresis is much smaller if the maximum value of I is smaller than Icr_2 (Figure 4, dotted line). The corresponding dependence for the fully equilibrated system reveals no hysteresis (Figure 4, dashed line).

Comparison with Experiment. We have carried out some straightforward experiments aimed at revealing the role of nonlinear dynamic effects in isolated photosynthetic RCs from the purple bacterium *R. sphaeroides* (wild-type). The isolation procedure and sample preparation are described elsewhere.[44]

The experimental conditions were pH = 7.5 at room temperature, and the buffer used was 20 mM Tris-HCl with 0.025% lauryldimethylamine *N*-oxide (LDAO) concentration. The RC suspension, with absorbance $A_{802} = 0.8$, was investigated in a 1-cm-path length cuvette. We followed the RC's optical absorbance changes in the maximum of the bacteriochlorophyll dimer P absorption band ($\lambda = 865$ nm). The testing light intensity was 10^9 quanta/(cm^2 s). Additional continuous wave excitation was provided by an incandescent lamp filtered by an interference filter ($\lambda_m = 850$ nm). First the intensity of continuous wave excitation (actinic light) was increased from zero up to a maximum level I_{max} of 4×10^{14} quanta/(cm^2s), and then it was diminished back to the initial low level. The rate of actinic light intensity variation was slow enough to ensure quasi-stationary experimental conditions (for a more detailed description of the experimental setup and methods, see ref 17).

The experiments showed hysteresis behavior in the optical absorbance ($\Delta A_{865}(I)$) that was proportional to the change of the overall number of photoexcited RCs (Figure 5, dots). The corresponding theoretical value can be defined as

$$\Delta A_{865} \approx \int_{-\infty}^{\infty} dx \, [n_A(x) + n_B(x)] P(x) \tag{23}$$

where $P(x)$ is determined from eqs 13 and 20−22; $n_A(I,x)$ and $n_B(I,x)$ are defined by eq 9.

The results of model calculations using the theory developed above for different sets of parameters (see the caption to Figure 5) are presented in Figure 5 (solid and dashed lines). The calculations reveal a broad bistability region. The width of the loop is in good agreement with the experimental results (Figure 5) and can be explained by the fact that a very small fraction of all RCs are switched into a new *conformational state* under the experimental conditions used (that is, the population $\nu 1$ of the first minimum of the conformational potential deviates only slightly from 1; see Figure 4, dashed line). The good match between the experimental and theoretical plots justifies the approach presented here. The most essential parameters influencing the theoretical curve $\Delta A_{865}/A_{865}$ are k_{AD}, x_0, k, and f_B. The dependencies depicted in Figure 5 were obtained for two sets of parameters: (1) $k_{AD} = 13$, $x_0 = 1$, $k = 0.5$, and $f_B = 7$ (the solid line) and (2) $k_{AD} = 6$, $x_0 = 1$, $k = 1.8$, and $f_B = 10$ (the dashed line). The corresponding variations of ΔG_{AB} calculated from $x|_{x=\chi} = \Delta G_{AB}/k_BT$ for these two cases (at room temperature) are (1) from 25 to ca. 300 meV and (2) from 25

to ca. 165 meV upon actinic light intensity variation from 0 up to some high, close to saturating, level. The first set of parameters gives a much better match of the theory to the experiment, but it requires a considerably larger variation of ΔG_{AB} as a function of the variation of the activating light intensity. We should note that the shape of the theoretical hysteresis curve depends strongly on the parameters that determine both the adiabatic potential and the RCs distribution function, i.e., k and f_B. This means that the choice of a potential of a different type (Lennard-Jones, Morse, or any other unharmonic potential) could improve the description considerably, even for small variations of the ΔG_{AB} value. This exemplifies the importance of determining the exact shape of the potential experimentally.

We know of no published experiments aimed specifically at studying light-induced ΔG_{AB} changes. The estimates presented in different papers give values from 10 to 100 meV for ΔG_{AB} variation with both k_{AB} and k_{BA} variation and for different external conditions.[36,40] Such a variation of ΔG_{AB} is more than sufficient to cause the hysteresis behavior in our model, although the shape of the hysteresis loop obtained theoretically for such parameters differs significantly from experiment. We expect that the application of an adiabatic potential of a nonparabolic type in the theory would provide a closer correspondence between the theoretical and the experimentally observed hysteresis curves for the variation of ΔG_{AB} over the range from 10 to 100 meV. To make such an improvement to the theory, however, one should know the exact shape of the conformational potential. This very important information can be obtained, in principle, from a detailed experimental study of RCs, including the study of recombination kinetics under different conditions of illumination. We have obtained preliminary results on the $P^+Q_B^-$ recombination kinetics in RCs subjected to prolonged illumination of high-intensity light (data not shown). These results provide clear evidence for largly different shapes of the conformational potential for RCs in the PQ_AQ_B, $P^+Q_A^-Q_B$, and $P^+Q_AQ_B^-$ states. The principal purpose of the present work has been to develop the theory and to study the role of the slow conformational variable on the RC functioning. The exact parameter values in the model and the proper shape of the potentials will have to be elaborated in a more detailed experimental study.

Conclusion

Our theoretical study reveals the importance of nonlinear dynamic effects (that is, in our case, the bifurcations of a particular macroscopic parameter) for the function of an ensemble of photosynthetic RCs. We have shown that an interaction between photoseparated charges and cofactor/protein conformation may cause pronounced nonlinearity in the dependencies of macroscopic RC parameters (optical absorbance) on the intensity of actinic light. The comparison of the theory with our experimental results is encouraging and reveals good agreement between theoretical and experimental optical absorbance changes. These results have been discussed in terms of variation of free energy difference ΔG_{AB} following the variation of actinic light intensity. The RC in the dark-adapted state was found to be characterized by a low ΔG_{AB} value, whereas higher values of ΔG_{AB} could be obtained after long enough time of illumination of the sample with actinic light of close to saturating intensity. The slow conformational changes caused mainly by the electron localization on Q_B appear to be completed during this period of time. We suggest that the characteristic relaxation time of the structural variable x under consideration is at least on the order of minutes or longer. The existence of such modes with relaxation times up to 15−20 min has, for example, been detected in photoacoustic studies of RCs from *R. sphaeroides* recently.[24]

The two *conformational states* described by lower and upper branches in Figure 5 play, indeed, an important role in the function of the RC. After prolonged light adaptation, i.e., after the transition to the upper branch of the bistability curve, the *conformational state* of all the RCs should become almost independent of the variation of the intensity of acting light, thus ensuring a stable regime of RC functioning. This regime corresponds to a dramatic increase in the ET rate constant $k_{AB}(x)$ and a corresponding decrease of the reverse rate constant $k_{BA}(x)$ as compared with their values in the dark-adapted state, which corresponds to the lower branch of the bistability curve.

Acknowledgment. We acknowledge Mr. M. Reus for isolating reaction centers, Prof. K. Schaffner for his support of this work, and Dr. J. P. Connelly for fruitful discussion of the results and text of the manuscript. A.G. thanks the Max-Planck-Gesellschaft and the Sonderforschungsbereich 189 (Heinrich-Heine Universität Düsseldorf) for providing a fellowship.

References and Notes

(1) Deisenhofer, J.; Epp, O.; Sinning, I. Michel, H. *J. Mol. Biol.* **1995**, *246*, 429.
(2) Allen, J. P.; Feher, G.; Yeates, T. O.; Rees, D. C.; Deisenhofer, J.; Michel, H.; and Huber, R. *Proc. Natl. Acad. Sci. U.S.A.* **1986**, *83*, 8589.
(3) Treutlein, H.; Schulten, K.; Brunger, A. T.; Karplus, M.; Deisenhofer, J.; Michel, H. *Proc. Natl. Acad. Sci. U.S.A.* **1992**, *89*, 75.
(4) Schulten, K.; Tesch, M. *Chem. Phys.* **1991**, *158*, 421.
(5) Shaitan, K. V.; Uporov, V.; Lukashev, E. P.; Kononenko, A. A.; Rubin, A. B. *Mol. Biol. (Moscow)* **1991**, *25*, 695.
(6) Yruela, I.; Churio, M.; Geusch, T.; Braslavsky, S.; Holzwarth, A. *J. Phys. Chem.* **1994**, *98*, 12789.
(7) Stowell, M. H. B.; McPhillips, T. M.; Rees, D. C.; Soltis, S. M.; Abresch, E. C.; Feher, G. *Science* **1997**, *276*, 812.
(8) Gardiner, C. W. *Handbook of Stochastic Methods*; Springer-Verlag: Berlin, 1985.
(9) Haken, H. *Synergetics—An Introduction*; Springer-Verlag: Berlin, 1978.
(10) Glansdorf, P.; Prigogine, I. *Thermodynamics Theory of Structure, Stability and Fluctuations*; Wiley: London, 1971.
(11) Nicolis, G.; Prigogine, I. *Selforganization in Nonequilibrium Systems*; Wiley: New York, 1977.
(12) Gushcha, A.; Dobrovolskii, A.; Kapoustina, M.; Privalko, A.; Kharkyanen, V. *Phys. Lett.* **1994**, *A191*, 393.
(13) Goushcha, A.; Kapoustina, M.; Kharkyanen, V. *J. Biol. Phys.* **1994**, *19*, 273.
(14) Christoforov, L. *Phys. Lett.* **1995**, *A205*, 14.
(15) Chinarov, V. A.; Gaididei, Yu. B.; Kharkyanen, V. N.; Sit'ko, S. P. *Phys. Rev.* **1992**, *A46*, 5232.
(16) Dobrovolskii, A.; Filippov, A.; Goushcha, A.; Privalko, A.; Kharkyanen, V. *J. Biol. Phys.* **1994**, *19*, 285.
(17) Goushcha, A.; Kharkyanen, V.; Holzwarth, A. *J. Phys. Chem.* **1997**, *101*, 259.
(18) Dobrovolskii, A.; Filippov, A.; Goushcha, A.; Kapoustina, M.; Karataev, V.; Privalko, A.; Kharkyanen, V. *J. Biol. Phys.* **1995**, *21*, 265.
(19) Goushcha, A.; Berezetska, N.; Kapoustina, M.; Kharkyanen, V. *J. Biol. Phys.* **1996**, *22*, 113.
(20) Goushcha, A. O.; Bösinger, C. S.; Kharkyanen, V. N.; Holzwarth, A. R. *J. Phys. Chem.*, submitted.
(21) Risken, H. *The Fokker−Planck Equation*; Springer: Berlin, 1984.
(22) Gardiner, C. W. *Handbook of Stochastic Methods for Physics, Chemistry and the natural sciences*; Springer-Verlag: Berlin, 1985.
(23) Feller,W. *An introduction to probability theory and its applications*, 2nd ed.; Wiley: New York, 1974.
(24) Puchenkov, O. V.; Kopf, Z.; Malkin, S. *Biochim. Biophys. Acta.* **1995**, *1231*, 197.
(25) Kleinfeld, D.; Okamura, M. Y.; Feher, G. *Biochemistry* **1984**, *23*, 5780.
(26) Malkin, S.; Churio, M. S.; Shochat, S.; Braslavsky, S. E. *J. Photochem. Photobiol.* **1994**, *23*, 79.
(27) Mauzerall, D. C.; Gunner, M. R.; Zhang, J. M. *Biophys. J.* **1995**, *68*, 275.
(28) Marcus, R. A. *J. Chem. Phys.* **1956**, *24*, 966.
(29) Marcus, R. A.; Sutin, N. *Biochim. Biophys. Acta* **1985**, *811*, 265.
(30) Agmon, N.; Hopfield, J. J. *J. Chem. Phys.* **1983**, *78*, 6947.

(31) Haken, H.; *Light. Vol. 2. Laser Light Dynamics*; North-Holland: Amsterdam, 1985.

(32) Nienhaus, G. U.; Mourant, J. R.; Frauenfelder, H. *Proc. Natl. Acad. Sci. U.S.A.* **1992**, *89*, 2902.

(33) Schoepp, B.; Parot, P.; Lavorel, J.; Vermeglio, A. In *The Photosynthetic Bacterial Reaction Center II*; Breton, J., Vermeglio, A., Eds. Plenum Press: New York, 1992; pp 331−339.

(34) Wraight, C. A. *Biochim. Biophys. Acta* **1979**, *459*, 309.

(35) Kleinfeld, D.; Okamura, M. Y.; Feher, G. *Biochim. Biophys. Acta.* **1984**, *766*, 126.

(36) McComb, J. C.; Stein, R. R.; Wraight, C. A. *Biochim. Biophys. Acta* **1990**, *1015*, 156.

(37) Beroza, P.; Fredkin, D. R.; Okamura, M. Y.; Feher, G. *Proc. Natl. Acad. Sci. U.S.A.* **1991**, *88*, 5804.

(38) Beroza, P.; Fredkin, D. R.; Okamura, M. Y.; Feher, G. *Biophys. J.* **1995**, *68*, 2233.

(39) Gao, J.-L.; Shopes, R. J.; Wraight, C. A. *Biochim. Biophys. Acta.* **1991**, *1056*, 259.

(40) Okamura, M. Y.; Feher, G. *Annu. Rev. Biochem.* **1992**, *61*, 861.

(41) Wraight, C. A. *Isr. J. Chem.* **1981**, *21*, 348.

(42) Nonella, M.; Schulten, K. *J. Phys.Chem.* **1991**, *95*, 2059.

(43) Zusman, L. D. *Chem. Phys.* **1980**, *49*, 295.

(44) Müller, M. G.; Griebenow, K.; Holzwarth, A. R. *Chem. Phys. Lett.* **1992**, *199*, 465.

(45) This is supported also by the recent X-ray structural studies of RCs from *R. sphaeroides* made under different illuminating conditions[7] which appeared after submission of this paper. The authors observed a large light-induced shift and rotation of ubiquinone in the Q_B binding pocket from its equilibrium position in the dark. No significant light-induced structural changes have been observed in the Q_A binding pocket.